COMMUNICATION

ChemComm
www.rsc.org/chemcomm

Molecular satellite dishes: attaching parabolic and planar arenes to heterofullerenes†

Frank Hauke,[a] Stefan Atalick,[b] Dirk M. Guldi,*[b] James Mack,[c] Lawrence T. Scott*[c] and Andreas Hirsch*[a]

[a] *Institut für Organische Chemie, Henkestrasse 42, D-91054 Erlangen, Germany.*
E-mail: hirsch@organik.uni-erlangen.de
[b] *Radiation Laboratory, University of Notre Dame, Notre Dame, IN 46556, USA. E-mail: guldi.1@nd.edu*
[c] *Department of Chemistry, Merkert Chemistry Center, Boston College, Chestnut Hill, MA 02467-3860, USA. E-mail: lawrence.scott@bc.edu*

Received (in Cambridge, UK) 15th December 2003, Accepted 28th January 2004
First published as an Advance Article on the web 23rd February 2004

The electrophilic attack of $C_{59}N^+$ on arenes such as pyrene, coronene and corannulene leads to the regioselective formation of fullerene conjugates, in which polycyclic aromatics are connected to the spherical heterofullerene by a single σ-bond.

We recently became fascinated by the idea of synthesising rigid molecular architectures in which the spherical framework of a fullerene is directly connected to polycyclic aromatics such as coronene and corannulene (Fig. 1). These systems resemble molecular counterparts of satellite dishes connected to a spherical body. Evaluation of the calculated electronic properties of these systems (see below), together with the fact that fullerenes and heterofullerenes are good acceptors within photoinduced electron- or energy-transfer events implied that this geometrical analogy is accompanied by a functional analogy.

A molecular architecture that involves just a polycyclic aromatic hydrocarbon and a fullerene core connected through a single bond is structurally impossible with isocyclic fullerenes such a C_{60}, since a highly reactive dangling bond would be left on the fullerene core. Among the available fullerenes, only the heterofullerene $C_{59}N$ allows the attachment of singly bonded addends. We have previously shown that electron-rich aromatics can be regioselectively attached to $C_{59}N$ *via* the C atom located α to N upon thermal cleavage of the interdimer bond of $(C_{59}N)_2$ (**1**), *in situ* oxidation leading to $C_{59}N^+$ and subsequent electrophilic aromatic substitution.[1]

The analogous treatment of **1** with 1 equiv. of pyrene, coronene or corannulene and 14 equiv. of *p*-TsOH at 150 °C in *o*-dichlorobenzene (ODCB) in a constant stream of air leads to the formation of dyads **2**–**4**, which were isolated after purification by HPLC (Cosmosil, toluene) in 18.2, 16.6 and 8.8% yield, respectively (HPLC purity >98% for **2**–**4**).‡ The corannulene–fullerene dyad **4** represents a particularly pleasing architecture, since the parabolic corannulene unit is a partial structure of the fullerene framework. In the dyads **2** and **3**, the only conformational freedom is rotation of the addend around the connecting σ-bond. In **4**, the inversion of the corannulene is another allowed dynamic process.[3] This is one of several reasons why the solubilities of **2**–**4** are considerably lower than those of other monomeric $C_{59}N$ adducts containing, for example, flexible tri(ethylene glycol) chains. The lowest solubility found was for **3**, where an effective π–π stacking interaction between the coronenes in the solid state is expected.

Fig. 1 Schematic representation of the unidirectional transduction of photonic energy from a parabolic corannulene antenna to the heterofullerene $C_{59}N$.

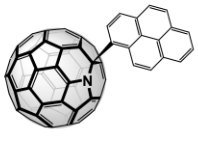

2

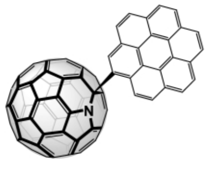

3

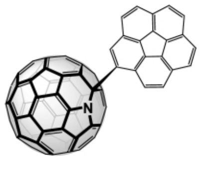

4

Since all protons are equivalent, substitution of one proton leads only to one adduct in the case of coronene and corannulene. Pyrene, on the other hand, has three different types of protons. The reaction with $C_{59}N^+$ yields exclusively 1-azafullerenylpyrene (**2**). Determination of the symmetry of the heterofullerene dyads **2**–**4** was carried out by ^{13}C and ^1H NMR analysis. The complete structural characterisation of **2**–**4** was done by ^1H NMR, ^{13}C NMR, UV/Vis and FT-IR spectroscopy, and by FAB mass spectrometry.

The electronic and anisotropic influence of the $C_{59}N$ core on the aromatic substituent can clearly be seen in the ^1H NMR spectra of the heterofullerene–arene dyads **2**–**4**. As an example, the ^1H NMR spectrum of the corannulene adduct **4** is depicted in Fig. 2.

In dyad **4**, the signals for all aromatic protons are shifted downfield (up to 2 ppm) compared to the parent corannulene (δ 7.82) due to the anisotropic and inductive influence of the heterofullerene unit. The singlet at δ 9.38 corresponds to proton H2, *ortho* to the azafullerenyl substituent. The doublet at δ 9.66 (^3J = 9.0 Hz) can be traced back to proton H10. Due to the coupling constant, the doublet due to proton H9 (δ 8.10) can be identified. Doublets due to protons H3 and H4 appear at δ 8.06 and 7.97 (^3J = 8.6 Hz), respectively. The rather large spatial distance between protons H5–H8 (δ 7.91, 7.89) and the heterofullerene core leads to only a small anisotropic shift for these protons.

The C_s symmetry of all three adducts can easily be derived from the ^{13}C NMR spectra of the corresponding compound. In the fullerene sp^2 region, 30 signals are observed: 28 signals show double intensity and two signals single intensity, as they belong to the *trans*-1 carbon atoms located on the mirror plane. By comparing

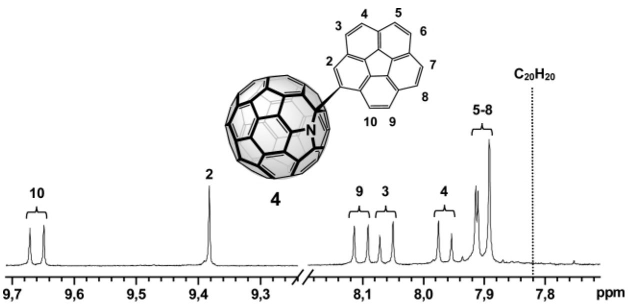

Fig. 2 ^1H NMR spectrum of azafullerenylcorannulene (**4**).

---

† Electronic supplementary information (ESI) available: PM3 calculations and molecular orbital diagrams for **2**–**4**. See http://www.rsc.org/suppdata/cc/b3/b316139k/

DOI: 10.1039/b316139k

the fullerene ^{13}C NMR signals of the dyads **2**–**4** with the signals of the parent arenes it is possible to separate the $C_{59}N$ resonances from the sp^2 signals of the aromatic moieties. The characteristic resonance of the sp^3 carbon atom of the heterofullerene cage can be detected in the region between δ 84 and 89.

Semiempirical calculations (PC Spartan Pro,[2] PM3; see ESI†) of the molecular orbitals of the dyads **2**–**4** show that the HOMO is centred on the arene subunit in the case of the pyrene adduct **2** and the coronene adduct **3**. In contrast to this result, the HOMO of azafullerenylcorannulene **4** is centred on the $C_{59}N$ core. The LUMO of all three dyads is $C_{59}N$-centred.

Insights into the electronic interaction between the $C_{59}N$ core and the respective arene moieties came from steady-state fluorescence spectroscopy. The fluorescence spectra of **2**–**4** in toluene are shown in Fig. 3. In particular, the arene emission—located predominantly in the visible region—is nearly quantitatively quenched. The respective arene quantum yields vary between 1.9×10^{-3} (pyrene dyad in toluene) and 7.1×10^{-4} (coronene dyad in benzonitrile). Parallel with the fluorescence quenching in the visible, we noted the appearance of the $C_{59}N$ emission in the near-infrared with a 825 nm maximum. Interestingly, the $C_{59}N$ fluorescence quantum yields match that determined for a reference under the same experimental conditions. Values around $(1.5 \pm 0.1) \times 10^{-4}$ illustrate this trend, despite the near exclusive excitation of the arene moieties. Additional excitation spectra of the $C_{59}N$ fluorescence, which reveal the ground-state transitions of the arenes, lead us to postulate an efficient and quantitative transfer of singlet excited-state energy from the highly energetic arene singlet excited state (~3.0 eV) to the low-lying singlet excited state of $C_{59}N$ (1.5 eV). Since the transduction of singlet excited states was found to be nearly quantitative in **2**–**4**, the change in HOMO location in **4**, that is, switched from the arene to the $C_{59}N$ core, does not lead to any notable differences in the excited-state deactivation.

In time-resolved fluorescence experiments, the only detectable fluorescence was that of the $C_{59}N$ core, whose lifetime (~1 ns) is, again, identical to that for the $C_{59}N$ reference carrying a tri(ethylene glycol)-substituted phenyl addend. No residual traces of the long-lived arene fluorescence—hundreds of nanoseconds in the references—were detected. This suggests that the strong $C_{59}N$–arene coupling features extremely fast intramolecular transfer dynamics (*i.e.* $> 10^{10}$ s^{-1}).

Transient absorption measurements corroborated the fluorescence experiments. Instead of seeing the arene singlet–singlet transitions (*i.e.* pyrene reference: absorption band in the spectral region around 480–550 nm), the transient spectra, recorded immediately after the 18 ps laser pulse, show mainly a broad 940 nm peak. The later maximum corresponds to the singlet–singlet fingerprint seen upon exclusive $C_{59}N$ excitation.[4] Again, the $C_{59}N$ singlet growth kinetics could not be resolved within our time resolution of ~20 ps. Once formed, the singlet–singlet transitions are metastable and decay with mono-exponential dynamics ($1.0 \pm 0.2 \times 10^9$ s^{-1}) to generate the triplet manifold.

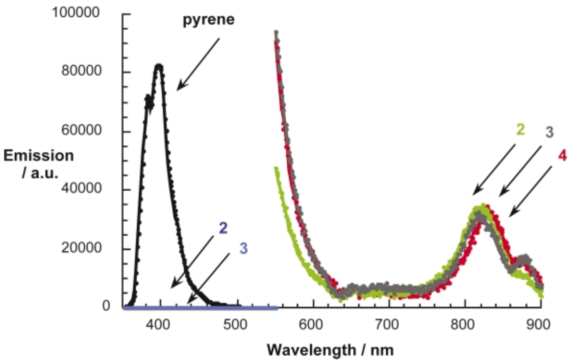

Fig. 3 Fluorescence spectra of pyrene reference and arene–$C_{59}N$ dyads **2**–**4**. Note that the NIR part is amplified by a factor of 300.

In conclusion, we have synthesised unique rigid molecular architectures in which polycyclic aromatics—satellite dishes—are directly connected to a spherical heterofullerene. Once photo-excited, the satellite dishes quantitatively transduce their photonic excited-state energy to the rigidly linked $C_{59}N$ moieties.

We thank the Deutsche Forschungsgemeinschaft DFG and the Graduiertenkolleg 'Homogener und heterogener Elektronentransfer' for financial support. Part of this work was supported by the Office of Basic Energy Sciences of the US Department of Energy (NDRL No. 4513 and DE-FG02–93ER14359)

Notes and references

‡ *Selected spectral data* for **2**: λ_{max}(ODCB)/nm, 337, 354, 442, 588 and 717; ^1H NMR (400 MHz, CS_2–$CDCl_3$) δ 10.53 (d, ^3J = 9.4 Hz, 1 H), 9.54 (d, ^3J = 8.2 Hz, 1 H), 8.57 (d, ^3J = 8.2 Hz, 1 H), 8.51 (d, ^3J = 9.4 Hz, 1 H), 8.37 (d, ^3J = 7.5 Hz, 1 H), 8.32 (d, ^3J = 7.5 Hz, 1 H), 8.26 (s, 2 H) and 8.14 (t, ^3J = 7.5 Hz, 1 H); ^{13}C NMR (100 MHz, CS_2–$CDCl_3$) δ 154.53 (2 C), 149.03 (2 C), 147.49 (1 C), 147.34 (2 C), 147.09 (2 C), 146.79 (2 C), 146.45 (2 C), 146.33 (2 C), 146.17 (2 C), 146.01 (2 C), 145.67 (2 C), 145.60 (1 C), 145.47 (2 C), 144.95 (2 C), 144.92 (2 C), 144.38 (2 C), 144.26 (2 C), 143.77 (2 C), 143.05 (2 C), 142.68 (2 C), 142.00 (2 C), 141.80 (2 C), 141.29 (2 C), 141.08 (2 C), 140.97 (2 C), 140.84 (2 C), 139.50 (2 C), 137.05 (2 C), 134.91 (2 C), 133.18 (1 C, ar), 132.65 (1 C, ar), 131.25 (1 C, ar), 130.60 (1 C, ar), 130.35 (1 C, ar), 128.96 (1 C, ar), 128.85 (1 C, ar), 128.60 (1 C, ar), 127.26 (1 C, ar), 126.38 (1 C, ar), 126.12 (1 C, ar), 126.05 (1 C, ar), 125.94 (1 C, ar), 125.19 (1 C, ar), 124.87 (2 C), 124.57 (1 C, ar), 124.21 (1 C, ar) and 84.61 (1 C, sp^3-C); MS (FAB) *m*/*z* 924 $[M]^+$ and 722 $[C_{59}N]^+$. For **3**: λ_{max}(ODCB)/nm 310, 348, 438 and 708; ^1H NMR (400 MHz, CS_2–$CDCl_3$) δ 11.47 (d, ^3J = 8.8 Hz, 1 H), 10.44 (s, 1 H), 9.37 (d, ^3J = 8.8 Hz, 1 H), 9.26 (d, ^3J = 8.5 Hz, 1 H), 9.09 (d, ^3J = 8.5 Hz, 1 H) and 9.03 (m, 6 H); ^{13}C NMR (100 MHz, CS_2–1-chloronaphthalene) δ 158.08, 152.57, 150.67, 150.52, 150.28, 150.04, 149.84, 149.49, 149.35, 149.19, 148.84, 148.74, 148.66, 148.13, 147.52, 147.40, 146.93, 146.18, 145.75, 145.13, 144.94, 144.47, 144.30, 144.15, 143.97, 142.77, 141.53, 140.25, 139.02, (further signals superposed by resonances of 1-chloronaphthalene) and 88.82 (1 C, sp^3-C); MS (FAB) *m*/*z* 1022 $[M]^+$ and 722 $[C_{59}N]^+$. For **4**: λ_{max}(ODCB)/nm 324, 442, 582 and 713; ^1H NMR (400 MHz, CS_2–$CDCl_3$) δ 9.66 (d, ^3J = 9.0 Hz, 1 H), 9.38 (s, 1 H), 8.10 (d, ^3J = 9.0 Hz, 1 H), 8.06 (d, ^3J = 8.6 Hz, 1 H), 7.97 (d, ^3J = 8.6 Hz, 1 H), 7.91 (d, 2 H) and 7.89 (s, 2 H); ^{13}C NMR δ(100 MHz, CS_2–$CDCl_3$) 154.18 (2 C), 148.76 (2 C), 147.47 (1 C), 147.27 (2 C), 1447.08 (2 C), 146.94 (2 C), 146.64 (2 C), 146.30 (2 C), 146.15 (2 C), 145.98 (2 C), 145.60 (2 C), 145.58 (1 C), 145.44 (2 C), 144.85 (2 C), 144.82 (2 C), 144.36 (2 C), 144.16 (2 C), 143.71 (2 C), 142.98 (2 C), 142.60 (2 C), 141.93 (2 C), 141.67 (2 C), 141.22 (2 C), 141.14 (2 C), 140.87 (2 C), 140.75 (2 C), 139.91 (1 C, ar), 139.53 (2 C), 137.07 (2 C), 136.53 (1 C, ar), 136.35 (1 C, ar), 136.26 (1 C, ar), 135.62 (1 C, ar), 135.54 (1 C, ar), 135.09 (2 C), 133.10 (1 C, ar), 131.28 (1 C, ar), 130.74 (1 C, ar), 130.42 (1 C, ar), 129.76 (1 C, ar), 128.82 (1 C, ar), 128.73 (1 C, ar), 128.57 (1 C, ar), 127.98 (1 C, ar), 127.78 (1 C, ar), 127.56 (1 C, ar), 126.95 (1 C, ar), 126.87 (1 C, ar), 126.63 (1 C, ar), 124.13 (2 C) and 83.54 (1 C, sp^3-C); MS (FAB) *m*/*z* 971 $[M]^+$ and 722 $[C_{59}N]^+$.

1 (*a*) B. Nuber and A. Hirsch, *Chem. Commun.*, 1998, 405; (*b*) F. Hauke and A. Hirsch, *Chem. Commun.*, 1999, 2199; (*c*) F. Hauke and A. Hirsch, *Tetrahedron*, 2001, **57**, 3697.
2 PC Spartan Pro, Molecular Modelling Package, Wavefunction Inc., Irvine, CA, USA.
3 L. T. Scott, M. M. Hashemi and M. S. Bratcher, *J. Am. Chem. Soc.*, 1992, **114**, 1920.
4 F. Hauke, A. Hirsch, S.-G. Liu, L. Echegoyen, A. Swartz, C. Luo and D. M. Guldi, *ChemPhysChem*, 2002, **3**, 195–205.